A Combined VUV Synchrotron Pulsed Field Ionization-Photoelectron and IR−VUV Laser Photoion Depletion Study of Ammonia†

Mi-Kyung Bahng, Xi Xing, Sun Jong Baek, Ximei Qian, and C. Y. Ng*

Department of Chemistry, University of California, Davis, One Shields Avenue, Davis, California 95616

Received: August 18, 2005; In Final Form: October 27, 2005

The synchrotron based vacuum ultraviolet-pulsed field ionization-photoelectron (VUV−PFI−PE) spectrum of ammonia (NH_3) has been measured in the energy range 10.12−12.12 eV using a room-temperature NH_3 sample. In addition to extending the VUV−PFI−PE measurement to include the $\upsilon_2^+ = 0$, 10, 11, 12, and 13 and the $\upsilon_1^+ + n\upsilon_2^+$ ($n = 4-9$) vibrational bands, the present study also reveals photoionization transition line strengths for higher rotational levels of NH_3, which were not examined in previous PFI−PE studies. Here, υ_1^+ and υ_2^+ represent the N−H symmetric stretching and inversion vibrational modes of the ammonia cation (NH_3^+), respectively. The relative PFI−PE band intensities for $NH_3^+(\upsilon_2^+=0-13)$ are found to be in general agreement with the calculated Franck−Condon factors. However, rotational simulation indicates that rotational photoionization transitions of the P-branches, particularly those for the lower υ_2^+ PFI−PE bands, are strongly enhanced by forced rotational autoionization. For the synchrotron based VUV−PFI−PE spectrum of the origin band of NH_3^+, rotational transition intensities of the P-branch are overwhelming compared to those of other rotational branches. Similar to that observed for the $n\upsilon_2^+$ ($n = 0-13$) levels, the $\upsilon_1^+ + n\upsilon_2^+$ ($n = 4-9$) levels are found to have a positive anharmonicity constant; i.e., the vibrational spacing increases as n is increased. The VUV laser PFI−PE measurement of the origin band has also been made using a supersonically cooled NH_3 sample. The analysis of this band has allowed the direct determination of the ionization energy of NH_3 as 82158.2 ± 1.0 cm^{-1}, which is in good accord with the previous PFI−PE and photoionization efficiency measurements. Using the known nd($\upsilon_2^+=1,1_0 \leftarrow 0_0$) Rydberg series of NH_3 as an example, we have demonstrated a valuable method based on two-color infrared−VUV−photoion depletion measurements for determining the rotational character of autoionizing Rydberg states.

I. Introduction

As a model system for the study of photoionization dynamics, ammonia (NH_3) has been the subject of numerous photoionization and photoelectron studies.[1−13] Using the single-photon vacuum ultraviolet (VUV) and multiphoton excitation pulsed field ionization-photoelectron (PFI−PE) method, rotationally resolved photoelectron spectra for the $\upsilon_2^+ = 1-9$ inversion or "umbrella" vibrational bands of $NH_3^+(\tilde{X}^2A_2'')$ have been reported previously.[3−6] These studies have provided a detailed picture on the photoionization dynamics of NH_3 and accurate ionization energies (IEs) and spectroscopic constants for NH_3^+-($\tilde{X}^2A_2''$;$\upsilon_2^+=1-9$). Furthermore, by combining the known transition energy for $\upsilon_2^+ = 1 \leftarrow \upsilon_2^+ = 0$, the study of Reiser et al. has allowed the indirect determination of the IE for NH_3.[4] The most precise IE for NH_3 of 82 158.751 ± 0.016 cm^{-1} was obtained recently from the analysis of Rydberg series resolved in the high-resolution PIE measurement by Seiler et al.[6] Interestingly, there was no report on the rotationally resolved VUV−PFI−PE spectrum of the origin band of NH_3^+. The lack of VUV−PFI−PE measurement for the origin band is in part due to the unfavorable Franck−Condon factor (FCF) for the photoionization transition. The only successful observation of the rotationally resolved origin band of $NH_3^+(\tilde{X}^2A_2'')$ was made by Dickinson et al. using the (2+1′) resonance-enhanced multiphoton mass-analyzed threshold ionization scheme via the $NH_3(\tilde{C}';\upsilon_2'=0)$ intermediate state.[7]

When a molecule is excited to a Rydberg state lying above its ionization threshold, it can decay via autoionization, predissociation, and/or fluorescence.[8] It is well-known that near resonance autoionization processes can affect the rotational transition intensities in PFI−PE spectra via channel interactions.[7,9] Thus, the study on autoionization mechanisms is essential for the understanding of molecular photoionization dynamics. Ashfold et al.,[10] Miller et al.,[11] and Bacon and Pratt[12] have performed extensive studies on the autoionization mechanisms of NH_3. Noordam et al.[13] have provided an intuitive picture for the competition between the three decay channels, field ionization, rotational autoionization, and predissociation, based on the line widths observed in field induced ionization measurements. Moreover, the detailed characterization of the quantum defects of autoionizing Rydberg series can give valuable insight into the character of the molecular orbital from which the photoelectron is produced.

In this article, we report three experiments aiming to provide additional details on the photoionization dynamics of NH_3. First, taking advantage of the broad tunability of the high-resolution VUV synchrotron radiation source at the Chemical Dynamics Beamline of the Advanced Light Source (ALS), we have recorded the VUV−PFI−PE spectra for the $\upsilon_2^+ = 0-13$ vibrational bands and the combination bands $\upsilon_1^+ + n\upsilon_2^+$ ($n = 4-9$) of NH_3^+ using an effusive NH_3 sample at room temperature, where υ_1^+ is the symmetric N−H stretching vibrational

† Part of the "Chava Lifshitz Memorial Issue".

* To whom correspondence should be addressed. E-mail: cyng@chem.ucdavis.edu.

10.1021/jp054672t CCC: $33.50
Published on Web 12/06/2005

mode. This study represents the first PFI−PE study to determine the relative intensities of these ν_2^+ vibrational bands for comparison with the FCF prediction. Furthermore, this experiment has allowed the examination of photoionization transition line strengths for the formation of higher rotational states of $NH_3^+(\nu_2^+)$ and the observation of the PFI−PE vibrational bands of NH_3^+ [$\nu_2^+ = 0$, 10−13 and $\nu_1^+ + n\nu_2^+$ ($n = 4-9$)] for the first time. We have also performed VUV laser based PFI−PE measurements of the $NH_3^+(\tilde{X}^2A_2'';\nu_2^+=0-3)$ vibrational bands using a supersonically cooled NH_3 sample for comparison with the VUV synchrotron based measurements. The VUV laser PFI−PE spectrum of the origin band thus measured has provided a direct determination of the IE(NH_3). The comparison of the VUV laser PFI−PE spectra with the corresponding synchrotron based VUV−PFI−PE spectra have also made possible a more precise energy calibration of the VUV synchrotron based PFI−PE spectra.

As demonstrated in recent IR−VUV studies,[14−17] the IR−VUV−PIE and IR−VUV−PFI−PE schemes have resulted in a significant simplification of the respective PIE and PFI−PE spectra for NH_3. Here, we report the comparison of the autoionizing Rydberg series of NH_3 near its ionization threshold observed in the VUV laser PIE measurement and those recorded using the IR−VUV laser PIE scheme. Most interestingly, the two-color IR−VUV−PIE measurement of the present study reveals IR−VUV-photoion depletion (IR−VUV−PID) signals of NH_3^+, demonstrating that the IR−VUV−PID scheme can be a valuable method for determining the rotational character of autoionizing Rydberg resonances observed in single-photon VUV−PIE studies. The IR−VUV−PID measurement can be considered as a variant of IR−UV pump probe methods such as resonant ion-dip IR spectroscopy,[18,19] which was first demonstrated[21] by Page et al.

The earliest IR-rovibration-selected and UV-resonance-enhanced multiphoton ionization study dates back to the work of Esherick and Anderson.[20]

II. Experiment

A. Synchrotron Based VUV−PFI−PE Measurements. The PFI−PE vibrational bands of $NH_3^+(\nu_2^+=0-13)$ were measured using the VUV photoelectron-photoion facility of the Chemical Dynamics Beamline at the ALS, which was operated in the multibunch mode (period = 656 ns, dark gap = 112 ns). The experimental setup and procedures were similar to those described previously.[22−24] In the present experiment, a 2400 lines/mm grating (dispersion = 0.64 Å/mm) was used to disperse the first-order harmonics of the undulator VUV beam with entrance-exit slit sizes in the range 30−100 μm. The dispersed VUV beam emerging from the monochromator was focused into the photoionization/photoexcitation (PI/PEX) region of the apparatus. All spectra were calibrated by using the PFI−PE bands for $Ne^+(^2P_{3/2,1/2})$, $Ar^+(^2P_{3/2,1/2})$, $Kr^+(^2P_{3/2,1/2})$, and $Xe^+(^2P_{3/2,1/2})$ obtained under the same experimental conditions. This energy calibration procedure is based on the assumption that the Stark shifts for the IE of NH_3 and the rare gases are identical. We note that this energy calibration procedure also assumes the linear energy extrapolation. Because the low end of the VUV energy range of interest here is nearly 2 eV lower than the IE of $Xe^+(^2P_{3/2})$, we expect that the linear extrapolation method carries a larger error limit than that of ±0.5 meV as achieved in previous studies.[22−24] As described below, the energy calibration of the synchrotron based VUV−PFI−PE measurements was improved in this study by using the VUV laser PFI−PE spectra for the $\nu_2^+ = 0-3$ bands of NH_3^+.

In the present PFI−PE measurement, the NH_3 sample (purity ≥99.99%, Aldrich) was introduced into the PI/PEX region as an effusive beam at room temperature. The density of the effusive beam at the PI/PEX region was estimated to be 10^{-3} Torr. The background pressure in the photoionization chamber was maintained at ≈2×10^{-6} Torr during the experiment. The PFI pulse (0.8−1.0 V/cm, 40 ns duration) was applied every synchrotron period at a delay of 10 ns with respect to the beginning of the dark gap. The VUV energy was scanned in step intervals of 0.2 meV. The counting time per data point varied in the range 5−15 s for different ν_2^+ bands.

B. Laser Based VUV−PFI−PE Measurements. The experimental procedures for VUV−PFI−PE measurements using the VUV laser photoion-photoelectron apparatus have been described in detail previously.[25,26] In brief, the apparatus consists of a pulsed (30 Hz) tunable VUV laser system, a pulsed molecular beam source, a time-of-flight (TOF) electron spectrometer for PFI−PE detection, and a TOF mass spectrometer for ion detection. The electron spectrometer and ion mass spectrometer are each equipped with a set of microchannel plates (MCPs). Tunable VUV laser radiation is generated by resonance enhanced four-wave difference-frequency mixing ($\omega_{vuv} = 2\omega_1 - \omega_2$) in a Kr gas cell via the Kr 4p → 5p′ transition at 98 855.06 cm^{-1} ($=2\omega_1$). The fixed UV frequency, ω_1, is generated by sum frequency mixing of the second harmonic frequency of an injection seeded Nd:YAG (355 nm) pumped dye laser output and the fundamental output (1064 nm) of the Nd:YAG pumped laser. The tunable visible frequency, ω_2 (spans the range 580−725 nm) is generated by another dye laser pumped by the 532 nm output of the same Nd:YAG laser. The optical bandwidth of the VUV radiation is measured to be 0.12 cm^{-1} (fwhm).

The NH_3 (purity ≥99.99%, Aldrich) sample is premixed with He in the 1:9 ratio to a total stagnation pressure of ≈1100 Torr prior to the expansion through a pulsed valve (nozzle diameter = 0.5 mm) operating at 30 Hz. The pulsed beam thus formed is skimmed by a conical skimmer before entering the PI/PEX region of the photoion−photoelectron apparatus. On the basis of spectral simulation of single-photon VUV laser PFI−PE spectra for the $\nu_2^+ = 0-3$ vibrational bands of $NH_3^+(\tilde{X})$, we estimate that the rotational temperature for NH_3 achieved in the supersonic expansion is ≈20 K.

For the PFI−PE detection, a dc field of 0.1 V/cm is applied to PI/PEX region to disperse prompt background electrons. In the present VUV−PFI−PE measurement, a PFI field of 0.3 V/cm is employed after a 1 μs delay with respect to the VUV laser pulse. The resulting PFI−PEs are detected by the electron MCP detector. The signals from the electron MCP are amplified before feeding into a boxcar integrator, which is interfaced to a personal computer. Two digital delay generators are used to control the timing sequence of turning on the molecular beam, the VUV laser, and the electric field pulse for PFI and electron detection.

C. VUV−PIE, IR−VUV−PIE and IR−VUV−PID Measurements. The VUV−PIE and the two-color IR−VUV−PIE and IR−VUV−PID measurements are made using the same VUV laser photoion-photoelectron apparatus as described in section II.B. The IR−VUV experiments use an additional Nd:YAG pumped IR-optical parametric oscillator/amplifier (IR−OPO/A) laser system (repetition rate = 15 Hz, pulse energy ≈5 mJ/pulse, optical bandwidth ≈0.25 cm^{-1}).[18−21] The IR laser beam is aligned to counterpropagate with the VUV laser beam to ensure the maximum spatial overlap of the two lasers. The application of the VUV photoionization laser is delayed with

respect to the firing of the IR laser by ≈50−100 ns. After a delay of 1 μs with respect to the VUV laser pulse, a dc field of ≈60 V/cm is used to extract photoions into the TOF mass spectrometer for detection by the ion MCP detector.

To detect the IR−VUV−PIE and IR−VUV−PID signals, the boxcar is set to collect NH_3^+ photoion signals at 30 Hz with the "toggle mode". Because the VUV beam is fired at 30 Hz and the IR is set at 15 Hz, the toggle mode allows shot-to-shot corrections of VUV-only photoion background by taking the differences of two adjacent ion signals as the net signals in the IR−VUV−PIE and IR−VUV−PID measurements. The net signals for IR−VUV−PIE measurements are positive signals, whereas the IR−VUV−PID peaks have negative intensities. In this work, the focus is on the demonstration of IR−VUV−PID measurements of the Rydberg series of NH_3.

The application of the IR−VUV−PIE and IR−VUV−PID method involves two steps. The first step concerns the measurement of the IR spectrum of neutral NH_3. This is done by scanning the IR laser radiation through rovibrational transitions from the ground vibrational state to the excited υ_1 (symmetric N−H stretch) = 1 vibrational state of NH_3 while fixing the VUV laser radiation at a frequency below the VUV photoionization threshold of NH_3. Because NH_3^+ can only be formed when NH_3 absorbs both the IR and VUV photons, the recorded IR−VUV-photoion spectrum for NH_3^+ corresponds to a measure of the IR absorption spectrum of NH_3, which provides accurate measures of the IR frequencies for the preparation of $NH_3(\upsilon_1=1)$ in specific rotational levels. From another point of view, setting the IR laser at a selected rotational transition also depletes the populations of specific rotational levels in the ground vibrational state of NH_3. Thus, fixing the IR frequency at a specific rotational transition and scanning the VUV laser energy can give rise to a negative PIE signal of an autoionizing Rydberg peak if the Rydberg line is formed by excitation from the neutral rotational state of NH_3, which is depleted by the IR radiation.

III. Symmetry Considerations and Selection Rules on NH_3 Photoionization

The selection rules based on symmetry considerations for the photoionization of NH_3 have been discussed in detail in refs 27−30. Here, only a brief summary is given to facilitate the interpretation of the current work. Ammonia in its ground $\tilde{X}^1A_1'$ state has a pyramidal structure of C_{3v} symmetry with the main electronic configuration of $(1a_1')^2(2a_1')^2(1e')^4(3a_1')^2$, whereas the $\tilde{X}^2A_2''$ ground state for NH_3^+ has a planar D_{3h} structure with the main electronic configuration of $(1a_1')^2(2a_1')^2(1e')^4(1a_2'')$.[27,28] Considering that the nuclear wave function in the ground state of NH_3 is located equally in both potential wells associated with the umbrella motion, NH_3 in its ground state can be considered to have D_{3h}(M) symmetry.[29] The inversion levels are labeled as the symmetric (A_2') and antisymmetric (A_2'') combinations of the C_{3v} pyramidal conformations interchanged through excitation of the inversion or "umbrella" mode.[30]

The selection rules for photoionization of NH_3 are governed by restrictions due to the nuclear spin statistics and by parity constraints.[28,29] On the basis of the nuclear spin statistics, the rovibronic levels with symmetries $\Gamma_{evr} = A_2$ for *ortho*-NH_3 and E for *para*-NH_3 have the nuclear spin statistical weights of 12 and 6, respectively, whereas no rovibronic levels with A_1 symmetry exist because of their zero statistical weights. In addition, transitions between levels of *ortho*-component and *para*-component are not allowed. The parity constraints on photoionization are described by $p_{evr}' \otimes p_{evr}^+ \otimes p_l = (-)$, where

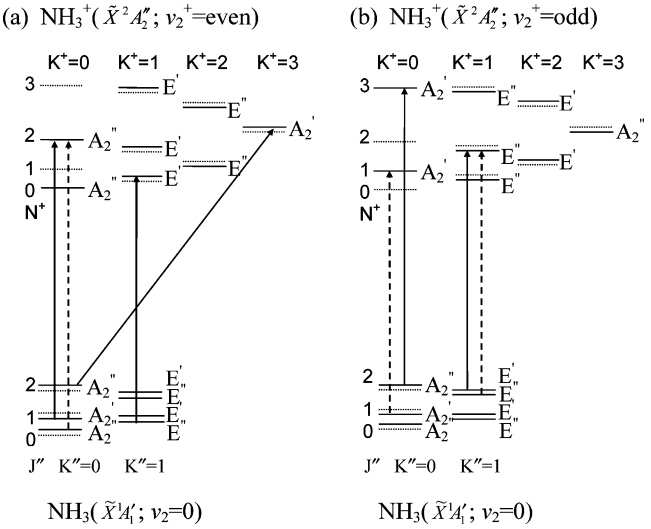

Figure 1. Symmetry labels of rotational energy levels for the $NH_3(\tilde{X}^1A_1';\upsilon_2=0)$ (lower) and $NH_3^+(\tilde{X}^+\,^2A_2'';\upsilon_2^+)$ (upper) states. Photoionization transitions to form $NH_3^+(\tilde{X}^+\,^2A_2'')$ in υ_2^+ = even states and υ_2^+ = odd states are shown in (a) and (b), respectively. Solid lines are allowed rotational levels and dotted lines are forbidden due to nuclear spin statistics. Some allowed transitions are shown as solid arrows for l even transitions and as dashed arrows for l odd transitions.

l is the orbital angular momentum quantum number of the photoelectron and $p_l = (-1)^l$ represents the photoelectron parity. From the combination of the two restrictions, allowed rovibronic transitions on the photoionization of NH_3 are as follows: $A_2' \leftrightarrow A_2''$ and $E' \leftrightarrow E''$ for even l, and $A_2' \leftrightarrow A_2'$, $A_2'' \leftrightarrow A_2''$, $E' \leftrightarrow E'$ and $E'' \leftrightarrow E''$ for odd l.

The schematic diagrams of Figure 1a,b show the symmetry labels of some rovibronic energy levels of the $NH_3(\tilde{X}^1A_1';\upsilon_1=0)$ and $NH_3^+(\tilde{X}^2A_2'';\upsilon_2^+)$ states and the symmetry allowed transitions between them, which are of interest to the present study. The respective rovibronic transitions to even ν_2^+ [Γ_υ(even υ_2^+) = A_1'] and odd υ_2^+ [Γ_υ(odd ν_2^+) = A_2''] are depicted separately in Figure 1a,b for the sake of clarity.

IV. Results and Discussion

A. VUV−PFI−PE Spectra for NH_3^+[υ_2 = 0−13 and $\upsilon_1^+ + n\upsilon_2^+$ (n = 4−9)]. Figure 2 depicts the single-photon VUV−PFI−PE spectrum of NH_3 in the energy range 10.13−11.90 eV obtained using an effusive NH_3 sample and the high-resolution monochromatized VUV undulator synchrotron source at the ALS. The energy range of this spectrum covers the formation of the vibrational bands of υ_2^+ = 0−13 and $\upsilon_1^+ + n\upsilon_2^+$ (n = 4−9). Particularly, this spectrum provides a grand view of the Franck−Condon envelope for photoionization transitions to these υ_2^+ vibrational bands of $NH_3^+(\tilde{X}^2A_2'')$ from the $NH_3(\tilde{X}^1A_1')$ ground state. The excitation profile of the long υ_2^+ vibrational progression observed in the VUV−PFI−PE spectrum is similar to that reported in previous HeI photoelectron measurements[1,31] and is consistent with the pyramidal-to-planar geometry change upon photoionization of NH_3. The υ_2^+ band intensity is found to increase from υ_2^+ = 0 to 5 and then decrease from υ_2^+ = 5 to 13. The υ_2^+ = 14 band is the last band that can be observed within the sensitivity of the present experiment. However, because no rotational structures are evident in the VUV−PFI−PE spectrum of this band, it is not shown here. The relative intensities for the υ_2^+ = 0−13 PFI−PE vibrational bands observed here are in general agreement with the FCFs calculated by Botschwina et al.[32]

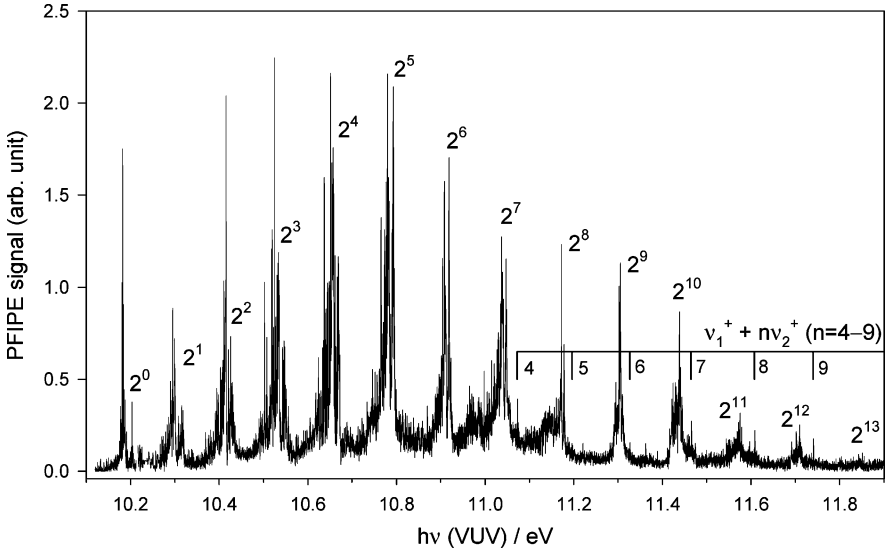

Figure 2. Synchrotron based VUV−PFI−PE spectrum of NH_3^+ in the VUV energy range 10.13−11.90 eV. The vibrational bands $\upsilon_2^+ = 0-13$ and $\upsilon_1^+ + n\upsilon_2^+$ ($n = 4$ and 9) are marked in the figure.

Parts a−l of Figure 3 compare the respective VUV−PFI−PE spectra for the $\upsilon_2^+ = 1-12$ bands of NH_3^+ (upper curves) with their corresponding simulated spectra (lower curves) obtained on the basis of the extended Buckingham−Orr−Sichel (BOS) model.[33−35] The assignments of rovibrational transitions are marked on top of the VUV−PFI−PE spectra. The spectrum for the ($\upsilon_2^+ = 0$ or 0^0) origin band of NH_3^+ along with its simulated spectrum is shown in Figure 4a.

The rotational structures of the PFI−PE vibrational bands of $NH_3^+(\upsilon_2^+=0-13)$ have been simulated by assuming that the energies $E_{J,K}$ ($E_{J^+K^+}$) for rotational levels of NH_3 (NH_3^+) are described by those of a rigid oblate symmetric top molecular species: $E_{J,K} = B_\upsilon J(J+1) + (C_\upsilon - B_\upsilon)K^2$ [$E_{J^+,K^+} = B_\upsilon^+ J^+(J^+ + 1) + (C_\upsilon^+ - B_\upsilon^+)(K^+)^2$], where $B_\upsilon(B_\upsilon^+)$ and $C_\upsilon(C_\upsilon^+)$ are the rotational constants and J (J^+) and K (K^+) are the rotational quantum numbers for a given vibrational level υ (υ^+) of NH_3 (NH_3^+). The rotational constants of the neutral ground vibrational state of NH_3, i.e., $\upsilon = 0$ or 0^0, $B_0 = 9.947$ cm^{-1} and $C_0 = 6.227$ cm^{-1}, are obtained from ref 30. The rotational constants (B_υ^+ and C_υ^+) for $NH_3^+(\upsilon_2^+=0-9)$ were taken from the ref 4. The B_υ^+ and C_υ^+ values for $\upsilon_2^+ = 10-13$ were determined by spectral simulations (see Table 1) of the present study. A Gaussian line shape with a full-width at half-maximum (fwhm) of 4.5 cm^{-1} is used as the instrumental PFI−PE resolution profile in the simulation.

The relative intensities for rotational structures observed in individual vibrational bands for $NH_3^+(\tilde{X}^2A_2'', \upsilon_2^+=0-13)$ were simulated using the extended Buckingham-Orr-Sichel (BOS) model as described in detail previously.[33−35] This model was originally derived to predict rotational line strength $\sigma(N^+\leftarrow J'')$ observed in single-photon photoionization of diatomic molecules[33] and has been extended for the simulation of symmetric top molecules.[34,35] Here, the BOS model is extended to simulate the rotationally resolved photoionization processes, $NH_3(\tilde{X}^1A_1'; 0^0, J, K) + h\nu \rightarrow NH_3^+(\tilde{X}^2A_2''; \upsilon_2^+=0-13, J^+, K^+) + e^-$, where both NH_3 and NH_3^+ are symmetric top species. The BOS model does not take into consideration of interchannel couplings and, thus, is not expected to be capable of providing a good fit to the PFI−PE spectrum if near resonance autoionization is an important photoionization mechanism. Despite this limitation, the BOS simulation has been shown to be useful for deducing more precise values for spectroscopic constants of interest such as IEs, vibrational frequencies, and rotational constants for the cation.[33−35] Furthermore, comparing the PFI−PE spectrum with its BOS simulation often helps to identify indirect photoionization processes mediated by near resonance autoionization.

On the basis of the BOS model, the photoionization cross section or line strength for a rotational photoionization transition is calculated according to

$$\sigma(N^+\leftarrow J'') \propto \sum_\lambda Q(\lambda, N^+, J'')C_\lambda \qquad (1)$$

The factor C_λ is associated with the electronic transition moment, which is the linear combination of electron transition amplitudes for the possible angular momentum l of the ejected electron. The other factor $Q(\lambda,N^+,J'')$ is determined by the standard angular momentum coupling constants (Clebsch−Gordon coefficients), which are calculated using the formula for a Hund's case (b) to case (b) transition in the present study and given by

$$Q(\lambda,N^+,J'') = (2N^+ + 1)\begin{pmatrix} N^+ & \lambda & J'' \\ -K^+ & K^+ - K'' & K'' \end{pmatrix}^2 \qquad (2)$$

where λ is the orbital angular momentum component out of which ionization occurs and is related to the quantum number l of the photoelectron by the relation $|\lambda - 1| \le l \le |\lambda + 1|$. Assuming that the highest occupied $3a_1'$ orbital of NH_3 is primarily atomic in nature, only the $\lambda = \pm 1$ transitions are included in the simulation. The calculation of the relative rotational transition intensities has also taken into account the Boltzmann rotational distribution of NH_3 at 298 K (room temperature) and the nuclear spin statistics of NH_3. Considering that the dominant feature of the spectra is governed by the P, Q, and R branches, and that the transitions involved are parallel type band transitions between the neutral and ion, we have only taken into account of the $\Delta J^+ = J^+ - J'' = 0, \pm 1$ and $\Delta K^+ = K^+ - K'' = 0$ transitions in the simulation. Although the rotational levels with the J'' values up to 15 and the K'' values up to 10 have been taken into consideration in the simulation, only $K'' = 0$ and 1 are marked in the assignments of Figure 3a−l and Figure 4a due to the space limitation.

All synchrotron based VUV−PFI−PE spectra for the $NH_3^+(\upsilon_2^+ = 1-12)$ bands are partially rotationally resolved with an intense Q-branch located at the center of each spectrum. As shown in Figure 3a−l, the pattern of rotational structures of

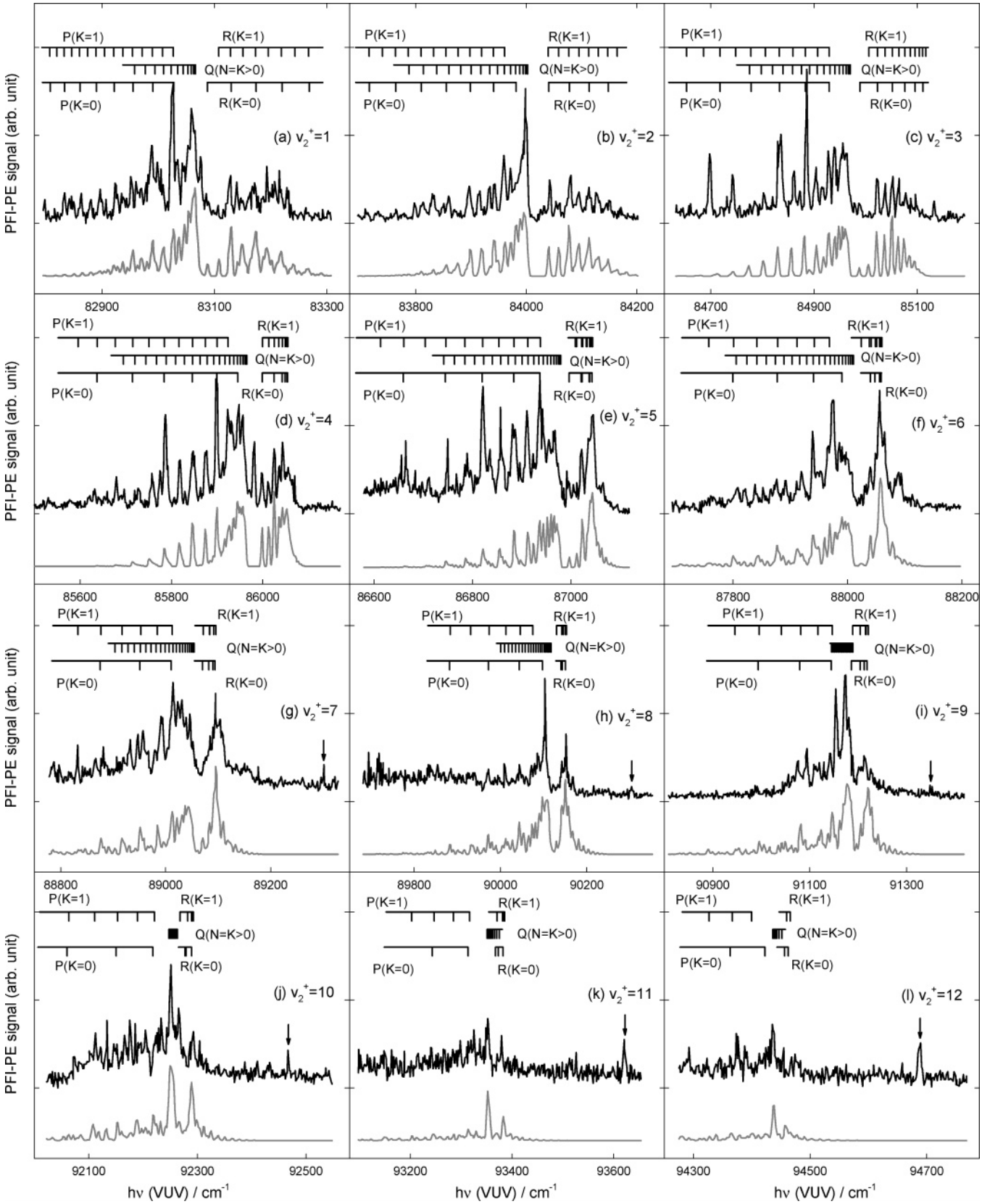

Figure 3. (a)−(l) are synchrotron based VUV−PFI−PE spectra of the 2^n (n = 1−12) vibrational bands of NH_3^+, respectively. Assignments of rotational photoionization transitions are marked on top of the peaks resolved in the spectra.

the simulated spectra (lower spectra) are in general agreement with those of the experimental spectra (upper spectra). A noticeable difference between the experimental and simulated spectra is that the P-branches of most of these PFI−PE vibrational bands, particularly the bands with lower v_2^+ values, exhibit strongly enhanced intensities for rotational transitions compared to the corresponding simulated intensities for these rotational transitions. This observation can be ascribed to forced autoionization[9,36] (an electron is released as a result of a channel interaction between a discrete Rydberg state and a pseudo-

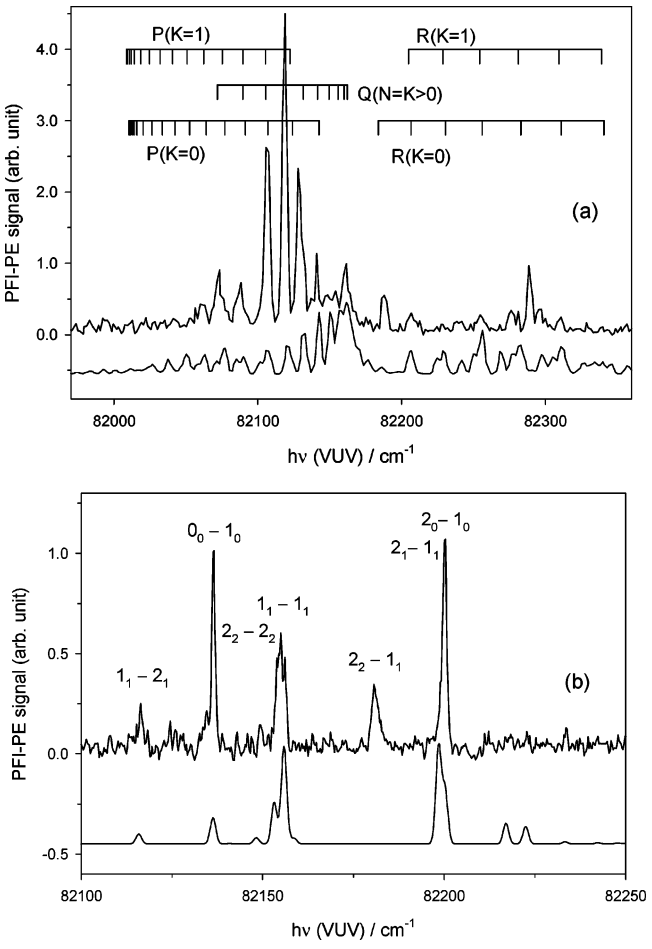

Figure 4. (a) Synchrotron based VUV−PFI−PE spectrum (upper spectrum) of the origin ($\upsilon_2^+ = 0$) band of NH_3^+ observed using a room-temperature NH_3 sample. (b) VUV laser based PFI−PE spectrum (upper spectrum) of the origin ($\upsilon_2^+ = 0$) band of NH_3^+ observed using a supersonically cooled NH_3 sample. Assignments of rotational photoionization transitions are marked on top of the peaks resolved in the spectra. The simulated spectra based on the extended BOS model are shown as the lower spectra in (a) and (b). See the text.

continuum of high-n Rydberg states and the subsequent field ionization of these high Rydberg states), which has been observed in PFI−PE vibrational bands of many simple molecular ions such as NO^+ [37] and ND_3^+.[24] The VUV−PFI−PE peaks (marked by downward arrows) on the high energy sides of the $\upsilon_2^+ = 7-12$ vibrational bands shown in Figures 3g−l are identified as the combination bands of $\upsilon_1^+ + n\upsilon_2^+$, $n = 4-9$, respectively. To show the relative intensities of these combination vibrational bands, we have also marked the $\upsilon_1^+ + n\upsilon_2^+$ ($n = 4-9$) bands in Figure 2, along with the marking of the $\upsilon_2^+ = 0-13$ vibrational progression.

As a result of forced rotational autoionization,[9,36] the synchrotron based PFI−PE spectrum of the origin band of NH_3^+ (shown in Figure 4a) is found to exhibit overwhelming intensities for the P-branch rotational transitions compared to the rotational transition intensities observed for other branches. The unusually high rotational intensities observed for the P-branch of the origin band are likely the result of longer lifetimes of Rydberg states involved near the ionization threshold of NH_3.

We have also obtained the VUV laser PFI−PE spectra for the $NH_3^+(\upsilon_2^+=0-3)$ vibrational bands using a supersonically cooled NH_3 sample. Considering that the VUV laser energy calibration can be made with significantly higher precision, we have used these VUV laser based spectra to recalibrate the energy scale of the VUV synchrotron based PFI−PE spectra. The VUV laser PFI−PE spectrum for the origin ($\upsilon_2^+ = 0$) band of NH_3^+ obtained here is plotted in Figure 4b for comparison with the synchrotron based spectrum of Figure 4a. Because the laser based PFI−PE spectra for the $\upsilon_2^+ = 1-3$ bands have been reported previously,[4−6] they are not shown here. Due to the significantly lower rotational temperature (≈20 K) achieved for the molecular beam NH_3 sample, the VUV laser PFI−PE spectrum for the origin band of NH_3^+ is found to display well resolved rotational transitions. The respective assignments of rotational transitions, $N^+_{K^+} \leftarrow J''_{K''}$, are marked on top of the PFI−PE peaks of Figure 4b. At a rotational temperature of 20 K, the NH_3 sample is predominantly populated in the 1_0 and 1_1 rotational levels. Because the BOS simulation model used here has assumed only the occurrence of $\Delta K^+ = 0$ transitions, the $\Delta K^+ = 1$ transition $2_2 \leftarrow 1_1$ observed in PFI−PE spectrum of

TABLE 1: Ionization Energies (IEs) and Rotational Constants (B_v^+/C_v^+) Observed in the Present VUV Synchrotron and Laser PFI−PE Measurements and Their Comparison with Previous UV and IR−VUV Laser PFI−PE Studies.

	IE (cm^{-1})				B_v^+/C_v^+ (cm^{-1})	
ν^+ bands	VUV synchrotron[a]		ref 4[b]	VUV[c] or IR−VUV[d]	ref 4[b]	VUV[c] or IR−VUV[d]
2^0	82162	905[e]	82159.0	82158.2	10.64/5.25	10.64/5.10
2^1	83067	935[e]	83062.4	83061.6	10.19/5.31	10.18/5.27
2^2	84002	968[e]	84002.9	84002.9	9.77/5.40	9.76/5.39
2^3	84970	995[e]	84972.2	84972.3	9.35/5.50	9.33/5.46
2^4	85965	1014[e]	85966.4	85965.6	8.95/5.60	8.95/5.53
2^5	86979	1031[e]	86980.2	86979.5	8.60/5.70	8.57/ -
2^6	88010	1044[e]	88010.7		8.25/5.80	
2^7	89054	1063[e]	89058.4		7.95/5.95	
2^8	90117	1072[e]	90116.8		7.65/6.05	
2^9	91189	1078[e]	91189.4		7.40/6.20	
2^{10}	92267	1088[e]				7.15/6.35
2^{11}	93355	1087[e]				6.90/6.50
2^{12}	94442	1090[e]				6.65/6.65
2^{13}	95532					6.40/6.80
1^12^1			86501.0	86285.7	9.9/5.25	10.00/5.60
1^12^3				88180.7		9.23/−
1^12^4	89301[f]	1004[g]				
1^12^5	90305[f]	1047[g]				
1^12^6	91352[f]	1115[g]				
1^12^7	92467[f]	1154[g]				
1^12^8	93621[f]	1068[g]				
1^12^9	94689[f]					

[a] This work. Based on VUV synchrotron based PFI−PE measurements. The IE values are obtained on the basis of BOS simulations of the VUV synchrotron based PFI−PE spectra and are estimated to have error limits of ±5 cm^{-1} for $\upsilon_2^+ = 0-11$ and ±8 cm^{-1} for $\upsilon_2^+ = 12$ and 13. The simulations of the VUV synchrotron based PFI−PE spectra for the $\upsilon_2^+ = 0-9$ bands use B_v^+/C_v^+ values reported in ref 4. For the $\upsilon_2^+ = 10-13$ bands, the B_v^+/C_v^+ values are determined on the basis of the best simulated fit to the VUV synchrotron based PFI−PE spectra and the extrapolation of the B_v^+/C_v^+ values for the $\upsilon_2^+ = 0-9$ bands of ref 4. [b] The IE and B_v^+/C_v^+ values for the $\upsilon_2^+ = 0-9$ and $\upsilon_1^+ + \upsilon_2^+$ vibrational bands are obtained from ref 4 on the basis of nonresonant two-photon PFI−PE and (2+1′) resonant multiphoton PFI−PE measurements. [c] The IE and B_v^+/C_v^+ values for $\upsilon_2^+ = 0-3$ are determined on the basis of simulation of the VUV laser PFI−PE spectra obtained in the present work. The IE and B_v^+/C_v^+ values for $\upsilon_2^+ = 10-13$ are determined on the basis of simulation of the VUV synchrotron PFI−PE spectra obtained in the present work. [d] The IE and B_v^+/C_v^+values for $\upsilon_1^+ + n\upsilon_2^+$ ($n = 1$ and 3)are obtained from the IR−VUV−PFI−PE study reported in ref 38. [e] Vibrational spacings of adjacent υ_2^+ vibrational levels. [f] The IE values of the combination bands $\upsilon_1^+ + n\upsilon_2^+$ ($n = 4-9$) are estimated as the energies of the VUV−PFI−PE peaks marked as downward arrows in Figures 3g−l. See the text. [g] Vibrational spacings of adjacent $\upsilon_1^+ + n\upsilon_2^+$ ($n = 4-9$) vibrational levels.

Figure 4b is not predicted in the lower simulated curve. The BOS simulation of Figure 4b has taken into account the spin-rotation splitting of 0.8 cm^{-1} for the neutral states and used a Gaussian instrumental profile of a fwhm $\approx$1.8 cm^{-1}. Similar to the observation in Figure 4a, the P-branch rotational transitions, $0_0 \leftarrow 1_0$ and $1_1 \leftarrow 2_1$ are also found to be enhanced by forced autoionization.

The simulation of the VUV laser PFI−PE spectrum of Figure 4b leads to the B_v^+/C_v^+ values of 10.64/5.10 cm^{-1} for the ground state of NH_3^+ and IE(NH_3) value of 82 158.2 $\pm$ 1.0 cm^{-1}. These values, together with B_v^+/C_v^+ and IE values for $v_2^+ = 1-3$ determined in the present VUV laser PFI−PE measurement and those for $v_2^+ = 4$ and 5 obtained in the recent IR−VUV−PFI−PE study,[38] are compared in Table 1 to those for $v_2^+ = 0-9$ reported previously by Reiser et al.[4] The IE(NH_3) = 82 158.2 $\pm$ 1.0 cm^{-1} determined here on the basis of simulation of the present VUV laser PFI−PE study is in excellent agreement with the previous indirect determination[4] of 82 159.0 $\pm$ 1.0 cm^{-1} and the most precise value of 82 158.751 $\pm$ 0.016 cm^{-1} derived from the analysis of Rydberg series resolved in the recent high-resolution VUV−PIE study.[6] Using the B_v^+/C_v^+ constants for $v_2^+ = 0-9$ reported in ref 4 and those for $v_2^+ = 10-13$ obtained by simulations in this work, we have obtained the IE values for the formation of $NH_3^+(v_2^+=0-13)$ based on BOS simulations of the VUV synchrotron PFI−PE spectra. This comparison shows that the IE[$NH_3^+(\tilde{X};v_2^+=0-9)$] values obtained in the present synchrotron and laser VUV−PFI−PE study and the recent IR−VUV−PFI−PE measurement are in agreement with those obtained by Reiser et al. after taking into account the experimental uncertainties.

The present VUV synchrotron PFI−PE measurements also provide information on the combination bands $v_1^+ + nv_2^+$ ($n = 4-9$) of NH_3^+, which are predicted to occur by the FCF calculations.[39] The energies of the PFI−PE peaks (marked by downward arrows in Figures 3g−l) are considered as the positions for Q-branch rotational transitions of the $v_1^+ + nv_2^+$ ($n = 4-9$) bands. Thus, these PFI−PE peak energies are listed in Table 1 as estimates of the IEs for the formation of NH_3^+-[$v_1^+ + nv_2^+(n = 4-9)$] from NH_3. The Q-branch assignment is based on the observation of the VUV−PFI−PE spectra of the nv_2^+ ($n = 1-13$) bands, which are found to peak predominantly at the Q-branch rotational photoionization transitions. The VUV−PFI−PE spectra of the nv_2^+ ($n = 1-13$) bands shown in Figure 3a−l also reveal that as n is increased, the Q-branch becomes more dominant. The IE and B_v^+/C_v^+ values for $v_1^+ + nv_2^+$ ($n = 1$ and 3) obtained from the previous IR−VUV−PFI−PE and UV laser PFI−PE measurements are also included in Table 1.

We find that the vibrational spacings of the $v_1^+ + nv_2^+$ ($n = 4-9$) levels are close to those of the nv_2^+ ($n = 0-13$) (see Table 1). Furthermore, both the nv_2^+ and $v_1^+ + nv_2^+$ vibrational progressions are found to exhibit positive anharmonicities; i.e., the vibrational spacing increased as n increased. The extrapolation of the observed combination bands, $v_1^+ + nv_2^+$ ($n = 4-9$), yields an intercept or v_1^+ value of 3261 $\pm$ 36 cm^{-1}, which is slightly higher than the extrapolated value of 3232($\pm$10) cm^{-1} based on the IR−VUV−PFI−PE data. Nevertheless, these extrapolated v_1^+ values are in agreement after taking into account the error limits of both experiments. We note that the spacing (1120 cm^{-1}) observed between the IE for $v_1^+ + 4v_2^+$ obtained here and that for $v_1^+ + 3v_2^+$ determined in the IR−VUV−PFI−PE study seems too high compared to the vibrational spacings observed for the higher levels. This observation suggests that the IE values for $v_1^+ + nv_2^+$ ($n = 4$ and 5) obtained here on the basis of the estimates of the Q-branch assignments are likely too high.

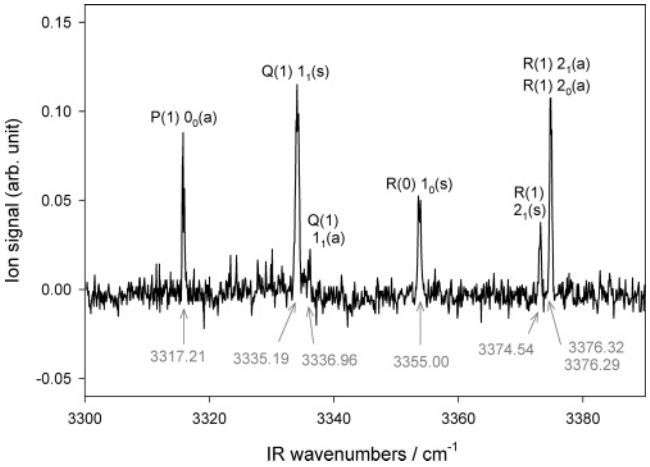

Figure 5. IR−VUV-photoion spectrum for the $v_1 = 1$ band of NH_3 in the IR frequency range 3300−3390 cm^{-1}. The VUV frequency was set at 82 057.5 and 82 049.1 cm^{-1} for measuring the IR spectrum in the regions of 3300−3320 and 3320−3390 cm^{-1}, respectively. The assignments of the rotational transitions are marked on top of the peaks resolved in the spectrum. The positions of these transitions are given below the peaks. See ref 38.

B. IR−VUV−PIE and IR−VUV−PID Spectra of NH_3^+. In this section, we present a valuable method for determining the rotational assignment of the autoionizing Rydberg series based on the two-color IR−VUV−PID scheme. Owing to the recent high-resolution PIE study of Seiler et al.,[6] several autoionizing Rydberg series converging to specific rotational levels of the excited $NH_3^+(v_2^+=1)$ vibrational state have been assigned. As described below, one of these Rydberg series of NH_3 is used here to illustrate the IR−VUV−PID technique for examining the rotational nature of autoionizing Rydberg states.

Figure 5 shows the IR−VUV-photoion spectrum for the v_1 band of NH_3 in the IR range 3300−3390 cm^{-1}. Although this spectrum was reported in the recent IR−VUV−PFI−PE study of NH_3,[38] it is shown again here to facilitate the description given below. This spectrum was obtained by detecting NH_3^+ ions with the VUV laser fixed at an energy below the IE(NH_3) while scanning the IR laser energy across the v_1 absorption band. Because NH_3^+ can be formed only when NH_3 absorbs both the IR and VUV photons, the IR−VUV-photoion spectrum thus obtained represents a measure of the IR absorption spectrum of NH_3. As shown in Figure 5, seven rotational transitions from $NH_3(v_1=0;J'',K'')$ to $NH_3(v_1=1;J',K')$ vibrational state are observed. These include the P(1) [0_0(a) $\leftarrow$ 1_0(s)] at 3317.21 cm^{-1}, Q(1) [1_1(s) $\leftarrow$ 1_1(a)] transition at 3335.19 cm^{-1}, Q(1) [1_1(a) $\leftarrow$ 1_1(s)] at 3336.96 cm^{-1}, R(0) [1_0(s) $\leftarrow$ 0_0(a)] at 3355.00 cm^{-1}, R(1) [2_1(s) $\leftarrow$ 1_1(a)] at 3374.54 cm^{-1}, R(1) [2_0(a) $\leftarrow$ 1_0-(s)] at 3376.29 cm^{-1}, and R(1) [2_1(a) $\leftarrow$ 1_1(s)] at 3376.32 cm^{-1}. Here, the rotational transitions are designated as $J'_{K'} \leftarrow J''_{K''}$. The symmetric and antisymmetric tunneling components (i.e., symmetric and antisymmetric combinations of the two localized nuclear wave functions) of NH_3 are labeled as (s) and (a), respectively. We note that the assignment of the observed rovibrational transitions was made on the basis of the high-resolution IR spectroscopic data of Benedict et al.[40]

On the basis of the assignment of the IR−VUV-photoion spectrum of Figure 5, the IR laser can be used to prepare NH_3 in a known rotational level of $NH_3(v_1=1)$, i.e., $J' = 0$ via P(1) [0_0(a) $\leftarrow$ 1_0(s)] at 3317.2 cm^{-1}, $J' = 1$ via R(0) [1_0(s) $\leftarrow$ 0_0(a)] at 3355.0 cm^{-1}, or $J' = 2$ via both R(1) [2_0(a) $\leftarrow$ 1_0(s)] and R(1) [2_1(a) $\leftarrow$ 1_1(s)] at 3376.3 cm^{-1}, prior to VUV−PIE or

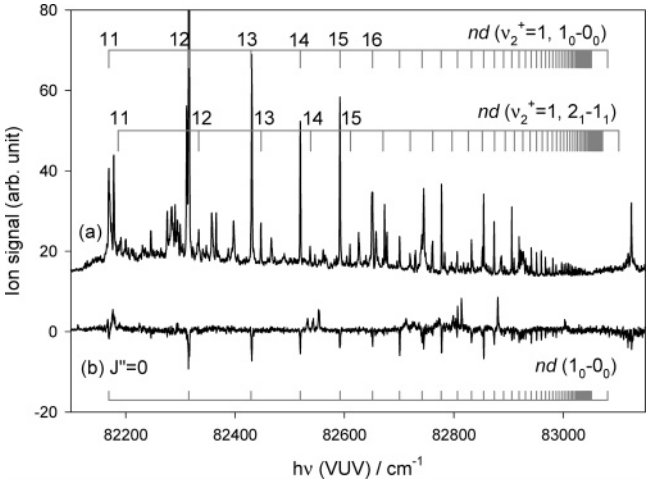

Figure 6. Upper spectrum: VUV−PIE spectrum of NH_3 in the VUV range 82 100−83 150 cm^{-1}. Lower spectrum: IR−VUV−PIE and IR−VUV−PID spectra of NH_3^+ observed by setting the IR laser at 3355.0 cm^{-1}, which corresponds to the R(0) [1_0(s) ← 0_0(a)] ($J'' = 0$) transition.

VUV−PFI−PE measurements. It has been demonstrated in previous IR−VUV studies[38] that the IR−VUV−PIE and IR−VUV−PFI−PE spectra can be greatly simplified due to the reduction of rotational photoionization transitions.

Figure 6 depicts the single-photon VUV−PIE spectrum (upper spectrum) of NH_3 in the VUV range 82 100−83 150 cm^{-1} obtained using a supersonically cooled NH_3 sample. This spectrum reveals complex autoionizing Rydberg structures and is consistent with the high-resolution VUV−PIE reported previously by Seiler et al.[6] As marked in Figure 6, the major autoionization features have been identified as members of two *n*d Rydberg series. The stronger Rydberg series, *n*d-(υ_2^+=1,1_0←0_0), has a quantum defect $\delta = 0.036$ and a converging limit of $NH_3^+(\tilde{X};\upsilon_2^+=1,J^+_{K^+}=1_0)$ at 83 082.2 cm^{-1}, and arises from the rotational transition $1_0 \leftarrow 0_0$. The weaker series, *n*d(υ_2^+=1,2_1←1_0), results from the rotational transition $2_1 \leftarrow 1_0$ and has a δ value of 0.055 and a converging limit of $NH_3^+(\tilde{X},\upsilon_2^+=1,J^+_{K^+}=2_1)$ at 83 102.3 cm^{-1}.

Using the "toggle" mode for NH_3^+ ion detection and setting the IR laser at the R(0) [1_0(s) ← 0_0(a)] ($J' = 1 \leftarrow J'' = 0$) transition, i.e., 3355.0 cm^{-1}, we have obtained the IR−VUV−PIE and IR−VUV−PID spectrum for NH_3^+ in the VUV range 82 050−83 250 cm^{-1} (see the lower spectrum of Figure 6). The positive IR−VUV−PIE signal corresponds to NH_3^+ formed from the intermediate state $NH_3[\tilde{X};\upsilon_1=1,1_0(s)]$ prepared by IR excitation, whereas the negative IR−VUV−PIE or IR−VUV−PID signal arises from depletion of the NH_3^+ ion intensity that results from photoionization of $NH_3[\tilde{X};\upsilon_1=0,0_0(a)]$. In other words, the observation of the IR−VUV−PID signal indicates that the autoionizing Rydberg resonance has a contribution from neutral $NH_3(\tilde{X};\upsilon_1=0)$ populating the 0_0(a) rotational level. As shown in Figure 6, the IR−VUV−PID spectrum exhibits a series of negative peaks, the positions of which match members of the *n*d(υ_2^+=1,1_0←0_0) Rydberg series observed in the upper VUV−PIE spectrum of NH_3. This observation can be taken as support for the assignment of this Rydberg series as originated from the 0_0(a) rotational level of $NH_3(\tilde{X};\upsilon_1=0)$.

As expected, the pattern of positive PIE peaks resolved in the lower IR−VUV−PIE spectrum of Figure 6 is significantly simplified compared to that observed in the upper VUV−PIE spectrum. However, the nature of these IR−VUV−PIE peaks is not known. Considering that the energy range for the IR−VUV−PIE spectrum of Figure 6 corresponds to the total energy (the sum of IR, VUV, and initial rotational energies of of NH_3) range 85 450−86 600 cm^{-1}, these IR−VUV−PIE peaks should belong mostly to members of the *n*d Rydberg series converging to $\upsilon_2^+ = 4$ and 5 states of NH_3^+ because the ionization thresholds for these states are 85 965.6 and 86 979.5 cm^{-1}, respectively.

We have also looked for IR−VUV−PID signals by setting the IR laser at 3317.2 cm^{-1} to excite the P(1) [0_0(a) ← 1_0(s)] transition and at 3376.3 cm^{-1} to excite both the R(1) [2_0(a) ← 1_0(s)] and R(1) [2_1(a) ← 1_1(s)] transitions. Due to the weak depletion signals observed for these measurements, the signal-to-noise ratios of these measurements are poor, and thus are not shown here.

V. Conclusions

We have obtained synchrotron based VUV−PFI−PE spectra for the $\upsilon_2^+ = 0-13$ vibrational bands of NH_3^+ using room-temperature NH_3. The higher rotational temperature of NH_3 has provided information on rotational photoionization transition line strengths for higher rotational states of NH_3, which were not observed in previous laser based PFI−PE studies. In addition to extending the rotationally resolved photoelectron measurement to higher vibrational bands $\upsilon_2^+ = 0$, 10−13, and thus, providing a grand view of the FCF profile for excitation of the υ_2^+ vibrational progression of NH_3^+, this experiment has also made possible the identification of the $\upsilon_1^+ + n\upsilon_2^+$ ($n = 4-9$) combination vibrational bands. Although the observed intensity profile of the υ_2^+ VUV−PFI−PE bands is in general agreement with the calculated FCFs, the P-branch rotational intensities for the origin VUV−PFI−PE band are found to be greatly enhanced by forced rotational autoionization, rendering a significantly higher overall intensity for the $\upsilon_2^+ = 0$ band than that predicted by the FCF calculation. We have also measured the VUV laser PFI−PE spectra for the $\upsilon_2^+ = 0-3$ bands of NH_3^+ using a supersonically cooled (≈20 K) sample. Simulation of the rotational structures resolved in the VUV laser PFI−PE spectrum of the origin band of NH_3^+ has provided a direct IE-(NH_3) determination of 82158.2 ± 1.0 cm^{-1}, which is in excellent accord with previous measurements.

Using the well-established autoionizing Rydberg series *n*d-(υ_2^+=1,1_0←0_0) of NH_3 as an example, we have demonstrated that the two-color IR−VUV−PID detection scheme is a valuable method for identifying the rotational nature of autoionizing Rydberg resonances.

Acknowledgment. C.Y.N. acknowledges the support by the NSF Grant No. CHE 0517871 and the U.S. Department of Energy Grant No. DE-FG02-02ER15306.

References and Notes

(1) Turner, D. M.; Baker, C.; Baker, A. D.; Brundle, C. R. *Molecular Photoelectron Spectroscopy*; Wiley-Interscience: London, 1970.

(2) Conaway, W. E.; Morrison, R. J. S.; Zare, R. N. *Chem. Phys. Lett.* **1985**, *113*, 429.

(3) Habenicht, W.; Reiser, G.; Müller-Dethlefs, K. *J. Chem. Phys.* **1991**, *95*, 4809.

(4) Reiser, G.; Habenicht, W.; Müller-Dethlefs, K. *J. Chem. Phys.* **1993**, *98*, 8462.

(5) Niu, B.; White, M. G. *J. Chem. Phys.* **1996**, *104*, 2136.

(6) Seiler, R.; Hollenstein, U.; Softley, T. P.; Merkt, F. *J. Chem. Phys.* **2003**, *118*, 10024.

(7) Dickinson, H.; Rolland, D.; Softley, T. P. *Philos. Trans. R. Soc. London, Ser. A* **1997**, *355*, 1585.

(8) Chupka, W. A.; Miller, P. J.; Eyler, E. E. *J. Chem. Phys.* **1988**, *88*, 3032 and references therein.

(9) Merkt, F.; Softley, T. P. *Int. Rev. Phys. Chem.* **1993**, *12*, 205.

(10) Ashfold, M. N. R.; Bennett, C. L.; Stickland, R. J. *Mol. Phys.*, **1987**, *19*, 181.

(11) Miller, P. J.; Chupka, W. A.; Eland, J. H. D. *Chem. Phys*. **1988**, *122*, 395.
(12) Bacon, J. A.; Pratt, S. T. *J. Chem. Phys.* **2000**, *112*, 4153.
(13) Warntjes, J. B. M.; Noordam, L. D. *J. Chem. Phys.* **2001**, *115*, 4150.
(14) Ng, C. Y. *J. Electron. Spectrosc. Relat. Phenom.* **2005**, *142*, 179.
(15) Woo, H. K.; Wang, P.; Lau, K.-C.; Xing, X.; Ng, C. Y. *J. Chem. Phys.* **2004**, *120*, 1756.
(16) Woo, H. K.; Wang, P.; Lau, K.-C.; Xing, X.; Ng, C. Y. *J. Phys. Chem. A* **2004**, *108*, 9637.
(17) Wang, P.; Xing, X.; Baek, S. J.; Ng, C. Y. *J. Phys. Chem. A* **2004**, *108*, 10035.
(18) Tanabe, S.; Ebata, T.; Fujii, M.; Mikami, N. *Chem. Phys. Lett.* **1993**, *215*, 347.
(19) Riehn, Ch.; Lahmann, Ch.; Wasswemann, B.; Brutschy, B. *Chem. Phys. Lett.* **1992**, *197*, 433.
(20) Esherick, P.; Anderson, R. J. M. *Chem. Phys. Lett.* **1980**, *70*, 621.
(21) Page, R. H.; Shen, Y. R.; Lee, Y. T. *J. Chem. Phys.* **1988**, *88*, 4621.
(22) Ng, C. Y. *J. Electron. Spectrosc. Relat. Phenom.* **2000**, *112*, 31.
(23) Jarvis, G. K.; Weitzel, K.-M.; Malow, M.; Baer, T.; Song, Y.; Ng, C. Y. *Rev. Sci. Instrum.* **1999**, *70*, 3892.
(24) Qian, X.-M.; Lau, K.-C.; He, G. Z.; Ng, C. Y.; Hochlaf, M. *J. Chem. Phys.* **2004**, *120*, 8476.
(25) Woo, H. K.; Zhan, J.; Lau, K.-C.; Ng, C. Y.; Cheung, Y.-S. *J. Chem. Phys*. **2002**, *116*, 8803.
(26) Woo, H. K.; Lau, K.-C.; Zhan, J.; Ng, C. Y.; Li, C. L.; Lee, W. K.; Johnson, P. M. *J. Chem. Phys.* **2003**, *119*, 7789.
(27) Herzberg, G. *Molecular Spectra and Molecular Structure, Vol. III, Electronic Spectra and Electronic Structure of Polyatomic Molecules*; Van Nostrand: Princeton, 1966.
(28) Bunker, P. R. *Molecular Symmetry and Spectroscopy*; Academic: New York, 1979.
(29) Signorell, R.; Merkt, F. *Mol. Phys*. **1997**, *92*, 793.
(30) Papoušek, D. *J. Mol. Struct*. **1983**, *100*, 179.
(31) Rabalais, U. W.; Karlsson, L.; Werme, L. O.; Bergmark, T.; Siegbahn, K. *J. Chem. Phys.* **1973**, *58*, 3370.
(32) Botschwina, P. In *Ion and Cluster Ion Spectroscopy and Structure*; Maier, J. P. Ed.; Elsevier: Amsterdam, 1989.
(33) Buckingham, A. D.; Orr, B. J.; Sichel, J. M. *Philos. Trans. R. Soc. London, Ser. A* **1970**, *268*, 147.
(34) Wang, K.; McKoy, V. In *High-Resolution Laser Photoionization and Photoelectron Studies*; Powis, I., Baer, T., Ng, C. Y., Ed.; Wiley: Chichester, U.K., 1995.
(35) Willitsch, S.; Hollenstein, U.; Merkt, F. *J. Chem. Phys.* **2004**, *120*, 1761.
(36) Garton, W. R. S.; Parkinson, W. H.; Reeves, E. M. *Proc. Phys. Soc. A* **1962**, *8*, 860.
(37) Jarvis, G. K.; Evans, M.; Ng, C. Y.; Mitsuke, K. *J. Chem. Phys.* **1999**, *111*, 3058.
(38) Bahng, M.-K.; Xing, X.; Baek, S. J.; Ng, C. Y. *J. Chem. Phys.* **2005**, *123*, 84311.
(39) Harshbarger, W. R. *J. Chem. Phys*. **1972**, *56*, 177.
(40) Benedict, W. S.; Plyler, E. K.; Tidwell, E. D. *J. Chem. Phys*. **1960**, *32*, 32.